Proc. Natl. Acad. Sci. USA
Vol. 91, pp. 3433–3437, April 1994
Microbiology

Borrelia burgdorferi swims with a planar waveform similar to that of eukaryotic flagella

(motility/periplasmic flagella/spirochetes)

STUART F. GOLDSTEIN*†, NYLES W. CHARON‡, AND JILL A. KREILING‡

*Department of Genetics and Cell Biology, University of Minnesota, St. Paul, MN 55108; and ‡Department of Microbiology and Immunology, P.O. Box 9177, Health Sciences Center, West Virginia University, Morgantown, WV 26506-9177

Communicated by Allan M. Campbell, November 1, 1993 (received for review August 10, 1993)

ABSTRACT **_Borrelia burgdorferi_ is a motile spirochete with multiple internal periplasmic flagella (PFs) attached near each end of the cell cylinder; these PFs overlap in the cell center. We analyzed the shape and motion of wild type and PF-deficient mutants using both photomicrography and video microscopy. We found that swimming cells resembled the dynamic movements of eukaryotic flagella. In contrast to helically shaped spirochetes, which propagate spiral waves, translating _B. burgdorferi_ swam with a planar waveform with occasional axial twists; waves had a peak-to-peak amplitude of 0.85 μm and a wavelength of 3.19 μm. Planar waves began full-sized at the anterior end and propagated toward the back end of the cell. Concomitantly, these waves gyrated counterclockwise as viewed from the posterior end along the cell axis. In nontranslating cells, wave propagation ceased. Either the waveform of nontranslating cells resembled the translating form, or the cells became markedly contorted. Cells of the PF-deficient mutant isolated by Sadziene _et al._ [Sadziene, A., Thomas, D. D., Bundoc, V. G., Holt, S. C. & Barbour, A. G. (1991) _J. Clin. Invest._ 88, 82–92] were found to be relatively straight. The results suggest that the shape of _B. burgdorferi_ is dictated by interactions between the cell body and the PFs. In addition, the PFs from opposite ends of the cell are believed to interact with one another so that during the markedly distorted nontranslational form, the PFs from opposite ends rotate in opposing directions around one another, causing the cell to bend.**

Spirochetes have several attributes that probably contribute to their ability to swim in gel-like media (1–6). Most—but not all (see below)—species are helical or have helical portions (4, 7); this morphology allows them to bore their way through these media in a corkscrew-like manner (1, 4). In addition, these bacteria have periplasmic flagella (PFs) between the outer membrane sheath and the cell cylinder (4, 7). Several lines of evidence indicate that the PFs are directly involved in motility (4, 8), and recent results with protruding PFs indicate that the PFs rotate similarly to the external flagella of rod-shaped bacteria (9–11). During translation, the PFs and cell body interact with one another and probably form a more rigid propeller than external flagella alone (1, 11, 12).

We report here that *Borrelia burgdorferi*, the causative agent of Lyme disease (13), swims by using helical PFs to produce a nonhelical cell shape. The PFs of *B. burgdorferi* are left-handed helices of defined helix pitch (1.48 μm) and diameter (0.28 μm) (10). Other spirochetes have been shown to have left-handed PFs but of different helix dimensions (10). *B. burgdorferi* has multiple PFs attached at each end that overlap in the cell center (13, 14). However, whereas most other spirochetes have cell bodies that are clearly helical, we report here that swimming cells of *B. burgdorferi* are planar. Moreover, cell translation is accomplished by producing posteriorly propagating planar waves resembling those found in eukaryotic flagella.

The publication costs of this article were defrayed in part by page charge payment. This article must therefore be hereby marked "*advertisement*" in accordance with 18 U.S.C. §1734 solely to indicate this fact.

MATERIALS AND METHODS

Organisms and Culture Conditions. Strains HB19, B31, and both avirulent and fresh isolates of strain 297 (fewer than three *in vitro* passages from hamsters) of *B. burgdorferi* were provided by R. C. Johnson (University of Minnesota, Minneapolis). The spontaneously occurring motility mutant of strain HB19 lacking PFs was provided by Alan Barbour (University of Texas, San Antonio) (8). Cells were grown in BSK medium at 35°C (15).

Light Microscopy. Approximately 5 μl of a cell suspension was placed on a slide and covered with a cover glass (22 × 22 mm) supported by a mixture of paraffin and Vaseline. For observations of cells swimming in methylcellulose, a drop of cells in culture medium was mixed on the slide with an approximately equal volume of 1% or 2% methylcellulose (2% = 4 $N \cdot s \cdot m^{-2}$ = 4000 cP; Matheson) in salts buffer (SB; 14.1 mM NaCl/12.6 mM $NaHCO_3$/5.4 mM KCl/1.5 mM $MgCl_2$/0.1 mM $CaCl_2$/46 mM Na_2HPO_4/3.5 mM NaH_2PO_4, pH 7.7). For measurements of swim speeds in a pure liquid, cells were centrifuged for 10 min at ≈745 × *g* at 4°C, rinsed twice in cold SB, and resuspended in the original volume of cold SB. Because cells in SB tended to adhere to glass, for measurements of swim speed, cell suspensions in SB were mixed on the slide with an approximately equal volume of a 1% solution of Ficoll (400 kDa; Sigma) in SB. This concentration of Ficoll slightly increases viscosity without producing a gel-like structure (3). More importantly, Ficoll inhibited the attachment of cells to the glass. To avoid surface effects related to cell motion, swim speeds were measured on cells translating at least a few micrometers from glass surfaces. Tethered cells were obtained either by using latex beads coated with antibody H6831 (16, 17) or by screening for cells spontaneously attached to the glass surface.

Photomicrography. Cell motions were recorded at room temperature, with either dark-field multiple-exposure photographs or video sequences and using either Zeiss or Leitz optics (12, 18). Multiple-exposure photographs displaying nonoverlapping images were taken with the film moving through the camera (18). Video sequences were taken in field mode with a model 72X CCD camera (DAGE–MTI, Michigan City, IN) and recorded in Super VHS with a model AG-6720A recorder (Panasonic). Either stroboscopic (18) or mercury arc lamp (12) illumination was used. As determined with a stage micrometer, the images were not reversed. Prints of video fields were made with a model UP-910 printer (Sony). Video sequences were taken with phase, dark-field, or Nomarski optics. Computer-assisted measurements of wave-

Abbreviations: PF, periplasmic flagellum; CCW, counterclockwise.

†To whom reprint requests should be addressed.

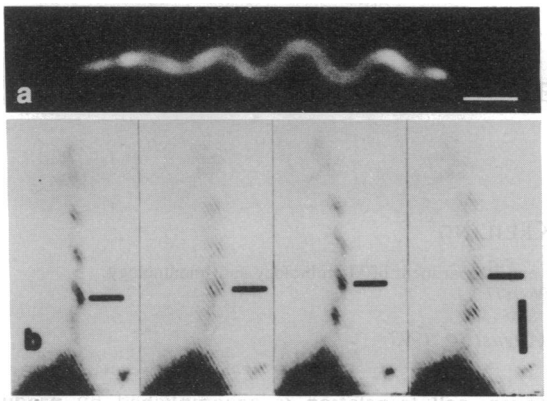

FIG. 1. Strain B31 in BSK medium. (*a*) Dark-field photograph of cell without protrusion. (*b*) Cell with protrusion. Reverse-contrast dark-field video fields showing progression of a wave away from the cell body. Line indicates same winding in each field. Interval between images, 1/60 s. (Bar = 2 μm.)

forms were made from video and multiple-exposure prints (12). Data points were spaced 0.15 μm apart. Measurements of swim speeds were made on the monitor screen from phase-contrast sequences. Results are expressed as means ± SD.

RESULTS

Swim Pattern. *B. burgdorferi* cells of all strains including fresh isolates often swam for a few seconds (exhibiting a "translational" form), stopped briefly (exhibiting a "non-translational" form), and resumed swimming in either the same or the reverse direction. Tethered cells exhibited patterns of stopping and starting similar to those of freely swimming cells and had similar waveforms. As with other bacteria, these tethered cells were more convenient to record and analyze for extended periods than cells that were swimming freely.

Motion of Protruding PFs. We have previously observed occasional protrusions on motile cells; these protrusions were composed of PFs surrounded by an outer membrane sheath; in other species these protrusions were found to rotate (10). We have now found that protrusions on *B. burgdorferi* also propagated waves, indicating rotation of the internal PFs (Fig. 1). Protrusions were rarely seen on strains 297 and HB19 but were frequently seen on strain B31.

Form of Translating Cells. The morphology of free-swimming translating cells and tethered cells was analyzed in detail. Cells looked the same in both methylcellulose and a pure liquid. Although we concentrated on nonvirulent strain 297, similar results were observed for strains B31, HB19, and fresh isolates of strain 297. Free-swimming translating cells and tethered cells exhibited a characteristic form. Several lines of evidence suggest that the cells had a flattened waveform rather than being a circular helix. First, the waveform could be oriented parallel (Fig. 2*a*), perpendicular (Fig. 2*b*), or oblique to the focal plane of the microscope. When a cell was oriented parallel to the focal plane, the entire waveform usually went in and out of focus as a unit as the plane of the microscope's focus was varied. Second, when the waveform was oriented perpendicular to the focal plane, the cell appeared as a line. Such cells had a beaded or a dashed appearance due to a series of alternating lighter and darker regions (Fig. 2*b*) rather than being a line of uniform density; a circular helix would appear as a series of slanted lines (19). Similar observations have been made on planar eukaryotic flagella (20). Finally, the length of the cell, as measured along the axis of the waveform, was the same whether the waveform was parallel to or perpendicular to the focal plane (Figs. 2 and 3). These results indicate that the observed variations of the waveform were not due to a periodic straightening and bending of the cell. However, occasionally (<5% of cells) a slight helical form was detected, and both right- and left-handed forms were observed. Even

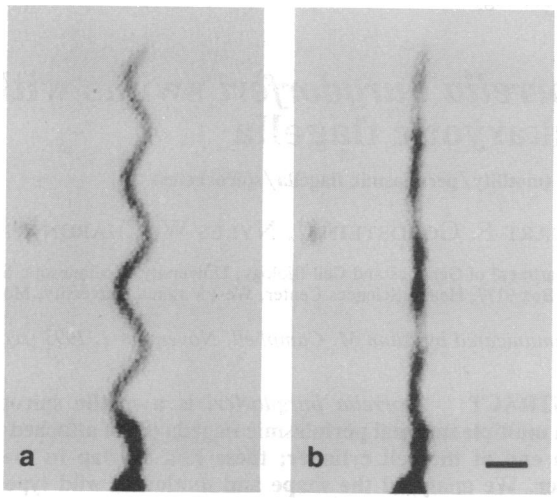

FIG. 2. Cell of strain 297 in 0.5% methylcellulose, tethered to a cover glass at end near bottom of figure. The cell is gyrating as waves propagate to bottom of figure. Cell is seen flat-on in *a* and edge-on in *b*. Axial length of cell is equal in all images. (Bar = 1 μm.)

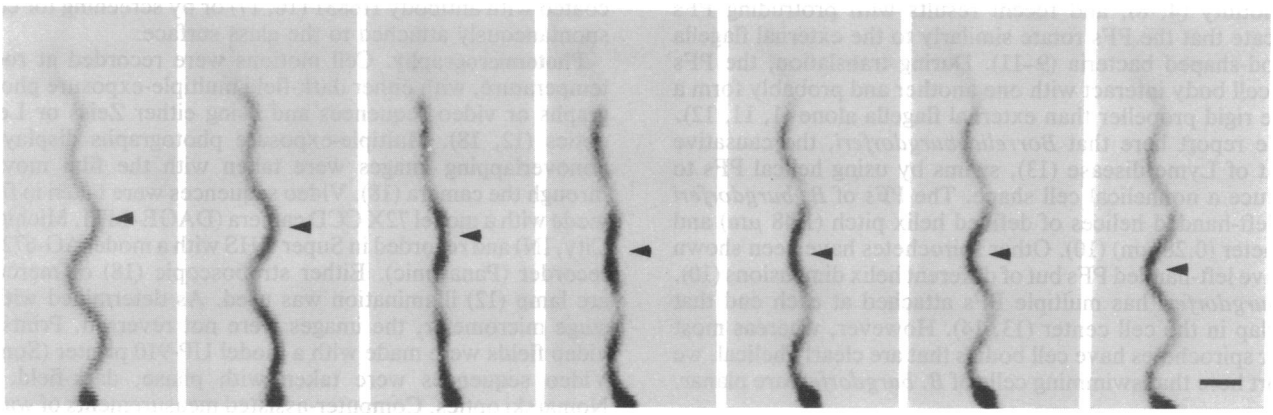

FIG. 3. Same cell as in Fig. 2. Waves are propagating toward bottom of figure. Bend indicated by arrowhead is moving from right to left. Focus is slightly above the cell, so that the bend is moving upward in the first three images and downward in the last three images. It is therefore rotating CCW as viewed from the bottom of the figure. (Bar = 1 μm.)

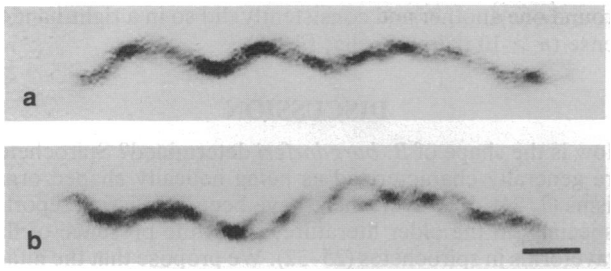

FIG. 4. Pair of intertwined cells of strain 297 in BSK medium. (*a*) Translating through medium. (*b*) Same pair a few seconds later, nontranslating, unwinding somewhat from one another. (Bar = 2 μm.)

when helicity was detectable, it was very slight and the cells were rather flat.

The translational waveforms were sinusoidal or meander-like and could be approximated by a series of circular arcs and straight connecting segments, as has been reported for eukaryotic flagella (21). The cells had the following dimensions: bend radius = 0.72 ± 0.11 μm (n = 66 bends on 13 cells); wavelength = 3.19 ± 0.34 μm (n = 56 bends on 13 cells); length (measured along the cell) per wavelength = 3.79 ± 0.46 μm (n = 56 bends on 13 cells); peak-to-peak amplitude = 0.85 ± 0.20 μm (n = 55 bend pairs on 13 cells); angle subtended by a bend = 1.54 ± 0.23 rad (n = 63 bends on 13 cells). Bend radius and wavelength could vary somewhat along a cell. This waveform was quite stable and was not dependent on concomitant cell motion. Cells incubated at 4°C for several hours were not motile but swam normally within an hour upon warming. Even when immobilized at 4°C, the cells exhibited this characteristic waveform. Waveforms generally appeared reasonably symmetrical. The cell axis was usually relatively straight, indicating that *B. burgdorferi* does not exhibit the pronounced principal/reverse bend-angle asymmetry often seen in eukaryotic flagella (22).

Cells did not always have flat waveforms over their entire length. Cells often had axial twists, so that different regions along a cell were in different planes. The positions and durations of these twists were quite variable; they could change rapidly. Occasionally, two adjacent swimming cells wrapped around one another and formed a double helix (Fig. 4*a*); these pairs of intertwined cells continued swimming and translating through the medium as a helical unit. When they intertwined, each cell wound around the other in the right-handed sense (n > 10 cells; data not shown). The winding period was 3.0 ± 0.4 μm (n = 7 pairs).

Wave Propagation of Translating Cells. Waves propagated along the cell from the anterior to the posterior end (Fig. 3). In contrast to waveforms of eukaryotic flagella (e.g., see ref. 23), propagating waves were full-sized at the anterior end instead of starting as small bends and increasing in size (Figs. 2 and 3). Beat frequencies of the fastest cells were 5–10 Hz in BSK medium.

A given cell usually gyrated as waves propagated along its length; i.e., the cell waveform turned about its axis as waves moved from the anterior to the posterior end. The direction of gyration could be determined by focusing above or below the cell axis and observing the apparent direction of movement of a wave. When focused above a cell, waves appeared to move from right to left, indicating that the cell was gyrating counterclockwise (CCW) as viewed from behind (Fig. 3). The frequency of gyration was quite variable but could approach the beat frequency.

The speeds of propagation of waveforms along cells were compared to the swim speeds. Cells with a beat frequency of 10.2 ± 1.0 Hz advanced at a speed of 4.25 ± 0.63 μm/s (n = 5 cells; mean wavelength = 3.35 μm) in SB containing 0.5% Ficoll. Waves propagated at a speed of 34.24 ± 5.44 μm/s relative to the cell (n = 5 cells). The ratio of swim speed to speed of wave propagation in these cells was 0.12 ± 0.02—i.e., in the time it took a wave to travel the length of a cell, the cell advanced 12% of its length through the medium.

Nontranslating Cells. The translation of a cell through the medium ceased while the propagation of waves from its anterior to its posterior end stopped. The duration of the nontranslational state was variable, from a tenth of a second or less to a few seconds. Nontranslating cells often appeared to freeze (data not shown). Cells also often exhibited marked shape changes when they stopped translating. In this form of flexing (1), the waves stopped propagating and the cell ends

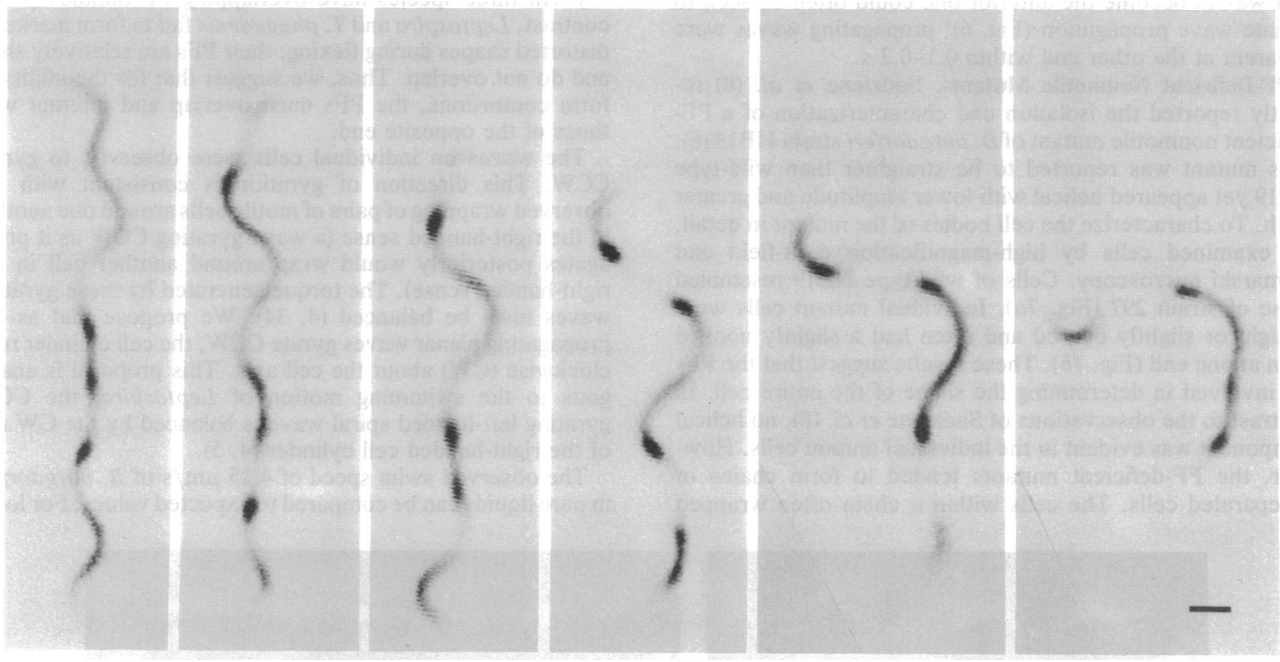

FIG. 5. Cell of strain 297 in BSK medium, tethered to the cover glass at bottom tip, undergoing extensive compressive shape change as it stops translating. Time elapsed = 5.3 s. (Bar = 1 μm.)

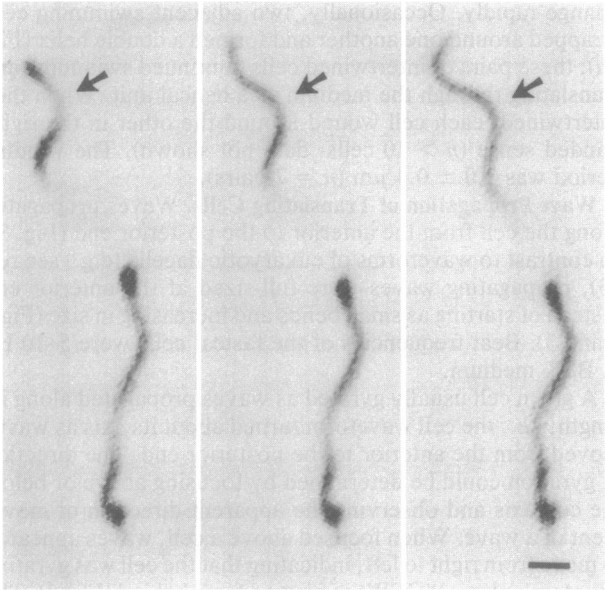

FIG. 6. Cell of strain 297 in BSK medium. Nontranslating cell beginning to resume translation toward top of figure. Propagation of waves is beginning at the anterior end (arrows), with no noticeable change at the other end. Interval between images, 1/60 s. (Bar = 1 μm.)

rapidly moved closer together (Fig. 5). The deformation could become extreme enough to produce a markedly distorted shape, causing the cell to bend in the midregion resembling a U shape (Fig. 5). These distorted cells appeared to retain some of the planar bends. Video sequences viewed in slow motion suggest that the changes in cell shape involved a relative gyration of the cell ends. Also, an apparent unwinding could be seen in pairs of intertwined cells, which, as noted above, assumed a helical form as they wound around one another. When translation stopped, these intertwined cells separated from one another as their helix diameters increased (Fig. 4*b*). As soon as waves began to be propagated along the cells, they resumed the translational mode. The end that was to become the anterior one could often be seen to initiate wave propagation (Fig. 6); propagating waves were apparent at the other end within 0.1–0.2 s.

PF-Deficient Nonmotile Mutants. Sadziene *et al.* (8) recently reported the isolation and characterization of a PF-deficient nonmotile mutant of *B. burgdorferi* strain HB19 (8). This mutant was reported to be straighter than wild-type HB19 yet appeared helical with lower amplitude and greater pitch. To characterize the cell bodies of the mutant in detail, we examined cells by high-magnification dark-field and Nomarski microscopy. Cells of wild-type HB19 resembled those of strain 297 (Fig. 7*a*). Individual mutant cells were straight or slightly curved and often had a slightly hooked form at one end (Fig. 7*b*). These results suggest that the PFs are involved in determining the shape of the entire cell. In contrast to the observations of Sadziene *et al.* (8), no helical component was evident in the individual mutant cells. However, the PF-deficient mutants tended to form chains of unseparated cells. The cells within a chain often wrapped around one another and consistently did so in a right-handed sense ($n > 10$ pairs of cells; Fig. 8).

DISCUSSION

How is the shape of *B. burgdorferi* determined? Spirochetes are generally characterized as being helically shaped organisms (7, 24). However, there have been conflicting reports, especially in the older literature, about the presence of flat waveforms in spirochetes (25–32). We propose that the intact *B. burgdorferi* cell conforms to its varied waveforms as a consequence of two different mechanical interactions. First, we suggest that the PFs interact with the cell cylinder. The motility mutant of Sadziene *et al.* (8) that lacks PFs had cell bodies that were relatively straight. Although it is conceivable that this mutant suffered a pleiotropic mutation, which altered both cell cylinder shape and PF synthesis, the results suggest that the PFs influence the shape of the entire cell. In addition, this hypothesis is consistent with models explaining the hook- and spiral-shaped ends of *Leptospira* (4, 5) and the bent-end morphology of *Treponema phagedenis* (11, 12). The PFs in these organisms are relatively short, do not overlap, and influence the shape of the cell in the specific domain where the PFs reside.

We propose that the second major type of interaction occurs between the two PF bundles. This interaction causes the shape of the cells to be altered and is most obvious during the flexing, which leads to the U-shaped form. Central to this hypothesis is the evidence that the PFs overlap in the midregion of the cell (14). Electron microscopy reveals that these overlapping PFs form a bundle and are not dispersed around the cell in the periplasmic space (14). Because *B. burgdorferi* PFs have a defined helix shape (10) and protrusions derived from the PFs propagate helical waves as do those of other spirochetes (10), the PFs apparently rotate. During flexing, we propose that the PFs from opposite ends wind around one another and rotate in opposing directions. Consequently, the cell is distorted, sometimes bending in the midregion and forming the U form. We have seen similar distortions in nontranslating cells of *Treponema pallidum* (N.W.C., S.F.G., and S. Norris, unpublished data), and similar forms have been reported in *Spirochaeta aurantia* (1, 33). All three species have overlapping PF bundles (7). In contrast, *Leptospira* and *T. phagedenis* fail to form markedly distorted shapes during flexing; their PFs are relatively short and do not overlap. Thus, we suggest that for the ability to form contortions, the PFs must overlap and interact with those of the opposite end.

The waves on individual cells were observed to gyrate CCW. This direction of gyration is consistent with the observed wrapping of pairs of motile cells around one another in the right-handed sense (a wave gyrating CCW as it propagates posteriorly would wrap around another cell in the right-handed sense). The torque generated by these gyrating waves must be balanced (4, 34). We propose that as the propagating planar waves gyrate CCW, the cell cylinder rolls clockwise (CW) about the cell axis. This proposal is analogous to the swimming motion of *Leptospira*: the CCW gyrating left-handed spiral wave is balanced by the CW roll of the right-handed cell cylinder (4, 5).

The observed swim speed of 4.25 μm/s of *B. burgdorferi* in pure liquids can be compared to expected values. For long,

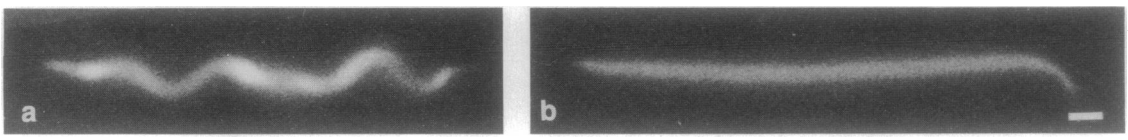

FIG. 7. Strain HB19 in growth medium. (*a*) Wild-type cell. (*b*) Mutant cell lacking PFs. (Bar = 1 μm.)

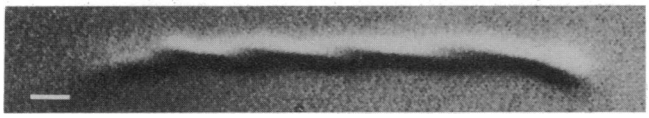

FIG. 8. Intertwined mutant cells of strain HB19 lacking PFs, wound around one another in the right-handed sense in growth medium. Focus is slightly above the cells. (Bar = 1 μm.)

thin cells, the ratio of swim speed (relative to the medium) to speed of wave propagation (relative to the cell) can be predicted for planar sine waves (35), planar meander-like waves consisting of circular arcs and straight segments (36), and helical waves (37). For an infinitely thin cell, the predicted values of swim speed/wave speed for the five cells whose speeds were measured are 0.21 ± 0.02 for a planar sine wave (35), 0.24 ± 0.02 for a planar meander-like wave (36), and 0.23 ± 0.02 for a circular helix (37). Assuming a diameter of 0.2 μm and a wavelength of 3.35 μm and using the correction of Cox (38) for cells of finite thickness as adapted by Chwang *et al.* (37) gives predicted values of swim speed/wave speed = 0.13 ± 0.01 for a planar meander-like wave (36) and 0.14 ± 0.01 for a circular helix (37). These latter estimates are in good agreement with the measured values of 0.12 ± 0.02. The similarity in the values predicted for planar and helical waveforms suggests that swim speed is not a major selective factor in the determination of cell shape. However, these calculations and measurements are for swimming in pure liquids, which may be different than the *in vivo* condition.

Kimsey and Spielman (6) have shown that the swim speed of *B. burgdorferi* increases markedly as the medium becomes more gel-like, as it does for other spirochetes (1). However, these authors report a swim speed of only 1.7 μm/s in growth medium. Their cells swam at 34.9 μm/s in 1% methylcellulose, indicating a wave speed of ≥34.9 μm/s. Assuming a similar wave speed and cell shape in growth medium, the expected swim speed would be ≈ 0.12 × 34.9 μm/s = 4.2 μm/s, which is similar to the results reported here. The reason for their low measured value in growth medium is not clear. However, *B. burgdorferi* can make frequent, brief stops without a change in cell shape, so that its average swim speed can be less than its swim speed during wave propagation. Because *B. burgdorferi* stops and reverses, care must be exercised in making speed measurements.

The waveform of *B. burgdorferi* resembles the waveforms of many eukaryotic flagella. Invertebrate sperm flagella typically have a flat meander-like waveform (21), as do many algal flagella (39) and some mammalian sperm tails (40, 41). *B. burgdorferi* and eukaryotic flagella both produce planar propagating waves but use very different mechanisms. *B. burgdorferi* generates traveling waves with rotary motors at the base of the PFs. Eukaryotic flagella propagate waves via microtubular sliding actively generated all along their length (e.g., see ref. 42). Indeed, planar propagating undulations of the sort seen in eukaryotic flagella require energy input all along the flagellar length (43). *B. burgdorferi* thus achieves a feat of which eukaryotic flagella are not capable: propagation of planar waves of constant amplitude along its entire length with energy input only in its terminal regions. Much remains to be learned about how *B. burgdorferi* is able to achieve this remarkable feat.

We thank R. C. Johnson for strains, encouragement, and help with cultures, and A. Barbour for strains and monoclonal antibodies. We appreciate the advice of S. Block concerning video equipment. This research was supported by Public Health Service Grant AI29743, and by a Grant-in-Aid from the University of Minnesota Graduate School.

1. Canale-Parola, E. (1978) *Annu. Rev. Microbiol.* **32,** 69–99.
2. Greenberg, E. P. & Canale-Parola, E. (1977) *J. Bacteriol.* **131,** 960–969.
3. Berg, H. C. & Turner, L. (1979) *Nature (London)* **278,** 349–351.
4. Goldstein, S. F. & Charon, N. W. (1988) *Cell Motil. Cytoskeleton* **9,** 101–110.
5. Berg, H. C., Bromley, D. B. & Charon, N. W. (1978) *Symp. Soc. Gen. Microbiol.* **28,** 285–294.
6. Kimsey, R. B. & Spielman, A. (1990) *J. Infect. Dis.* **162,** 1205–1208.
7. Canale-Parola, E. (1984) in *Bergey's Manual of Systematic Bacteriology*, eds. Krieg, N. R. & Holt, J. G. (Williams & Wilkins, Baltimore), pp. 38–70.
8. Sadziene, A., Thomas, D. D., Bundoc, V. G., Holt, S. C. & Barbour, A. G. (1991) *J. Clin. Invest.* **88,** 82–92.
9. Berg, H. C. & Anderson, R. A. (1973) *Nature (London)* **245,** 380–382.
10. Charon, N. W., Goldstein, S. F., Block, S. M., Curci, K., Ruby, J. D., Kreiling, J. A. & Limberger, R. J. (1992) *J. Bacteriol.* **174,** 832–840.
11. Charon, N. W., Greenberg, E. P., Koopman, M. B. H. & Limberger, R. J. (1992) *Res. Microbiol.* **143,** 597–603.
12. Charon, N. W., Goldstein, S. F., Curci, K. & Limberger, R. J. (1991) *J. Bacteriol.* **173,** 4820–4826.
13. Johnson, R. C., Schmid, F. W., Hyde, F. W., Steigerwalt, A. G. & Brenner, D. J. (1984) *Int. J. Syst. Bacteriol.* **34,** 596–597.
14. Hovind Hougen, K. (1984) *Yale J. Biol. Med.* **57,** 543–548.
15. Barbour, A. G. (1984) *Yale J. Biol. Med.* **32,** 818–824.
16. Barbour, A. G., Tessier, S. L. & Hayes, S. F. (1984) *Infect. Immun.* **45,** 94–100.
17. Charon, N. W., Daughtry, G. R., McCluskey, R. S. & Franz, G. N. (1984) *J. Bacteriol.* **160,** 1067–1073.
18. Goldstein, S. F. & Charon, N. W. (1990) *Proc. Natl. Acad. Sci. USA* **87,** 4895–4899.
19. Shimada, K., Kamiya, R. & Asakura, S. (1975) *Nature (London)* **254,** 332–334.
20. Gray, J. (1955) *J. Exp. Biol.* **32,** 775–801.
21. Brokaw, C. J. & Wright, L. (1963) *Science* **142,** 1169–1170.
22. Gibbons, B. H. & Gibbons, I. R. (1972) *J. Cell Biol.* **54,** 75–97.
23. Goldstein, S. F. (1977) *J. Exp. Biol.* **71,** 157–170.
24. Stephan, D. E. & Johnson, R. C. (1981) *Infect. Immun.* **32,** 937–940.
25. Schellack, C. (1908) *Arb. Kaiserl. Gesundh.* **27,** 364–387.
26. Neumann, F. (1929) *Klin. Wochenschr.* **8,** 2081–2085.
27. Pijper, A. (1949) *Symp. Soc. Gen. Microbiol.* **1,** 144–179.
28. Cox, C. D. (1972) *J. Bacteriol.* **109,** 943–944.
29. Jeantet, P. & Kermorgant, Y. (1925) *C. R. Sceances Soc. Biol. (Paris)* **92,** 1036–1038.
30. DeLamater, E. D., Wiggall, R. H. & Haanes, M. (1950) *J. Exp. Med.* **92,** 239–246.
31. Sequeira, P. J. L. (1956) *Lancet* **271,** 749 (and figure).
32. Jarosch, R. (1967) *Oesterr. Bot. Z.* **114,** 255–306.
33. Fosnaugh, K. & Greenberg, E. P. (1988) *J. Bacteriol.* **170,** 1678–1774.
34. Taylor, G. (1952) *Proc. R. Soc. London A* **211,** 225–239.
35. Gray, J. & Hancock, G. J. (1955) *J. Exp. Biol.* **32,** 802–814.
36. Brokaw, C. J. (1965) *J. Exp. Biol.* **43,** 155–169.
37. Chwang, A. T., Winet, H. & Wu, T. Y. (1974) *J. Mechanochem. Cell Motil.* **3,** 69–76.
38. Cox, R. G. (1970) *J. Fluid Mech.* **44,** 791–810.
39. Goldstein, S. F. (1992) in *Algal Cell Motility*, ed. Melkonian, M. (Chapman & Hall, New York), pp. 99–153.
40. Ishijima, S. & Mohri, H. (1985) *J. Exp. Biol.* **114,** 463–475.
41. Ishijima, S. & Witman, G. B. (1987) *Cell Motil. Cytoskeleton* **8,** 375–391.
42. Summers, K. E. & Gibbons, I. R. (1971) *Proc. Natl. Acad. Sci. USA* **68,** 3092–3096.
43. Machin, K. E. (1958) *J. Exp. Biol.* **35,** 796–806.